

Aberystwyth University

Bolla Bollana boulder beds

Le Heron, Daniel P.; Busfield, Marie E.; Collins, Alan S.

Published in:
Sedimentology

DOI:
[10.1111/sed.12082](https://doi.org/10.1111/sed.12082)

Publication date:
2014

Citation for published version (APA):

Le Heron, D. P., Busfield, M. E., & Collins, A. S. (2014). Bolla Bollana boulder beds: A Neoproterozoic trough mouth fan in South Australia? *Sedimentology*, 61(4), 978-995. <https://doi.org/10.1111/sed.12082>

General rights

Copyright and moral rights for the publications made accessible in the Aberystwyth Research Portal (the Institutional Repository) are retained by the authors and/or other copyright owners and it is a condition of accessing publications that users recognise and abide by the legal requirements associated with these rights.

- Users may download and print one copy of any publication from the Aberystwyth Research Portal for the purpose of private study or research.
- You may not further distribute the material or use it for any profit-making activity or commercial gain
- You may freely distribute the URL identifying the publication in the Aberystwyth Research Portal

Take down policy

If you believe that this document breaches copyright please contact us providing details, and we will remove access to the work immediately and investigate your claim.

tel: +44 1970 62 2400
email: is@aber.ac.uk



Bolla Bollana boulder beds: a Neoproterozoic trough mouth fan in South Australia

Journal:	<i>Sedimentology</i>
Manuscript ID:	SED-2013-OM-055.R1
Manuscript Type:	Original Manuscript
Date Submitted by the Author:	23-Jul-2013
Complete List of Authors:	Le Heron, Daniel; Royal Holloway, University of London, Earth Sciences Busfield, Marie; Royal Holloway, Earth Sciences Collins, Alan
Keywords:	trough mouth fan, Flinders Ranges, Sturtian, Neoproterozoic, Glaciation, snowball Earth, ice stream

1
2
3
4
5
6
7
8
9
10
11
12
13
14
15
16
17
18
19
20
21
22
23
24
25
26
27
28
29
30
31
32
33
34
35
36
37
38
39
40
41
42
43
44
45
46
47
48
49
50
51
52
53
54
55
56
57
58
59
60

1 **Bolla Bollana boulder beds: a Neoproterozoic trough**
2 **mouth fan in South Australia?**

3
4 DANIEL P. LE HERON^{*}, MARIE E. BUSFIELD^{*}, ALAN S. COLLINS[†].

5
6 ^{*}*Department of Earth Sciences, Queen's Building, Royal Holloway University of*
7 *London, Egham, TW200EX, United Kingdom*

8 [†]*TRAX, School of Earth and Environmental Sciences, University of Adelaide, SA*
9 *5005, Australia*

10
11
12 **Abstract**

13 The Bolla Bollana Formation is an exceptionally thick (~1500 m), rift-related
14 sedimentary succession cropping out in the northern Flinders Ranges, South Australia,
15 which was deposited during the Sturtian (mid Cryogenian) glaciation. Lithofacies
16 analysis reveals three distinct facies associations which chart changing depositional
17 styles on an ice-sourced subaqueous fan system. The diamictite facies association is
18 dominant, and comprises both massive and stratified varieties with a range of clast
19 compositions and textures, arranged into thick beds (1- 20 m), representing stacked,
20 ice-proximal glaciogenic debris flow (GDF) deposits. A channel belt facies
21 association, most commonly consisting of normally-graded conglomerates and
22 sandstones, displays scour and fill structure of ~10 m width and 1-3 m depth: these
23 strata are interpreted as channelised turbidites. Rare mud-filled channels in this facies
24 association bear glacially striated limestones. Finally, a sheet heterolithics facies
25 association contains a range of conglomerates through sandstones to silty shales
26 arranged into clear, normally graded cycles from the lamina to bed scale. These
27 record a variety of non-channelised turbidites, probably occupying distal and/or
28 interchannel locations on the subaqueous fan. Coarsening and thickening-up cycles,
29 capped by dolomicrites or mudstones, are indicative of lobe build out and
30 abandonment, potentially as a result of ice lobe advance and stagnation. Dropstones,
31 recognised by downwarped and punctured laminae beneath pebbles to boulders in
32 shale, or in delicate climbing ripple cross-laminated siltstones, are clearly indicative
33 of ice rafting. The co-occurrence of ice-rafted debris and striated limestones strongly
34 support a glaciogenic sediment source for the diamictites. Comparison to Pleistocene
35 analogues enables an interpretation as a trough mouth fan, most probably deposited
36 leeward of a palaeo-ice stream. Beyond emphasising the highly dynamic nature of
37 Sturtian ice sheets, these interpretations testify to the oldest trough-mouth fan
38 recorded to date.

39
40 **Keywords:** Sturtian; Neoproterozoic; Glaciation; snowball Earth; trough mouth fan;
41 ice stream; Flinders Ranges

INTRODUCTION

The northern Flinders Ranges of South Australia exposes an extremely thick succession of diamictites that were deposited during the Sturt glaciation (Young and Gostin, 1991; Preiss et al., 2011) at ~715 Ma (Macdonald *et al.*, 2010). In Arkaroola (**Fig. 1**), these deposits were first described by Mawson (1941, 1949), and interpreted as terrestrial glacial deposits. By contrast, glaciomarine interpretations were offered by Young and Gostin (1991) by the recognition of dropstone fabrics. The deposits are highly contentious and significant to debates focussed on the intensity and extent of Cryogenian glaciations (e.g. Fairchild and Kennedy, 2007; Etienne et al., 2007; Allen and Etienne, 2008), particularly as South Australia can be regarded as a type area for the “Sturtian” pan-glacial event (Hoffman and Schrag, 2002).

For some, scepticism surrounds the interpretation of many Cryogenian diamictite-bearing successions, such as those in the Flinders Ranges. A mechanism of diachronous rift shoulder glaciation, during the fragmentation of Rodinia, was proposed by Eyles and Januszczak (2004). In that model, debris flows were fluxed into rift basins. In Namibia, for example, it was proposed that some diamictites were deposited by non-glacially influenced gravity flow deposits (Eyles & Januszczak, 2007), amplifying Schermerhorn’s earlier non-glacial interpretations (Schermerhorn and Stanton, 1963; Schermerhorn, 1974). Such studies have hence stimulated questions about the clarity of the glacial signature in Neoproterozoic sedimentary successions. Recent examples worldwide, however, highlight the diverse range of reliable glaciogenic proxies preserved, despite tectonically active basin configurations (e.g. Arnaud, 2012; Busfield and Le Heron, in press; Le Heron et al., 2011, 2012; Uhlein et al. 2011). These studies provide substantive evidence for glacial processes

77 during the Neoproterozoic, irrespective of the scale of interpreted ice sheets (cf. Allen
78 and Etienne, 2008).

80 In this paper, a detailed facies analysis of the Bolla Bollana Formation in the
81 northern Flinders Ranges (**Fig. 1, 2**) is undertaken, presenting data from three
82 outstanding exposures. The succession is part of a classic diamictite succession which
83 has not been subjected to detailed investigation for over 20 years. The data were
84 collected as part of a six week field campaign in August 2012.

85
86
87 **STUDY AREA AND STRATIGRAPHY**

88 In the Arkaroola district of the northern Flinders Ranges, the lowermost of two
89 Neoproterozoic diamictite-bearing intervals is exposed. These rocks belong to the
90 Yudnamutana Subgroup (**Fig. 3**). A threefold subdivision of this subgroup is
91 recognised: the Fitton Formation occurs at the base, the Bolla Bollana Formation in
92 the middle, and the Lyndhurst Formation is the uppermost unit (**Fig. 3**). The Bolla
93 Bollana Formation was first examined in the Arkaroola district by Mawson (1941,
94 1949). This pioneering work offered a terrestrial glacial origin for the diamictites. The
95 formation itself was defined by Coats (in Thomson et al., 1964) as a subgreywacke
96 tillite of massive character with intercalated quartzite and siltstone. Young and Gostin
97 (1988, 1989, 1990, 1991) studied the Sturtian succession within the North Flinders
98 Basin (NFB), a sub-basin within the Adelaide Fold Belt that Preiss (1987, 1998, 2000)
99 argued was likely disconnected from depocentres in the central and southern Flinders
100 Ranges. Each paper presented a series of sedimentary logs, and facies descriptions,
101 recognising a comparable stratigraphic subdivision across the area. The dramatic
102 increase in knowledge of sedimentary processes at tidewater ice margins since the
103 time of Mawson motivated Young and Gostin (1989, 1991) to re-interpret the Bolla

1
2
3 104 Bollana Formation as glaciomarine. Regional mapping (Coats, 1973) demonstrates
4
5 105 that the Bolla Bollana Formation is extensive in the eastern part of the Copley Sheet,
6
7 106 and is particularly well exposed to the east and south of Arkaroola (**Fig. 1**).
8
9
10 107 Summarising the regional stratigraphy, Young and Gostin (1991) published a map
11
12 108 showing how sediment dispersal, surmised from a variety of palaeocurrent indicators,
13
14 109 testifies to the interplay of extensional tectonics, forming graben-like minibasins, and
15
16 110 palaeohighs (**Fig. 2**).
17
18
19 111

20
21 112 The Bolla Bollana Formation trends toward massive in character in the south
22
23 113 of the NFB, becoming stratified in the north. To explain this, Young and Gostin
24
25 114 (1988) suggested that ice-rafted debris (IRD) deposition was predominant in the
26
27 115 south, with reworking processes more important northward. No unequivocal glacially
28
29 116 striated surfaces are reported in Cryogenian successions of Australia, with the
30
31 117 exception of those in Western Australia (Corkeron, 2007). However, the “cast of
32
33 118 striations” is reported to occur “on the underside of basal Sturt silty mudstones near
34
35 119 Merinjina Well” (Young and Gostin, 1991). These were interpreted as tectonic by
36
37 120 Daily *et al.* (1973), and glaciogenic by others (Preiss, 1987; Young and Gostin, 1991;
38
39 121 Preiss *et al.*, 2011).
40
41
42 122

43
44
45 123 In our present paper, detailed facies descriptions and interpretations are
46
47 124 provided from three new sections at Stubb’s Waterhole, Tillite Gorge, and Weetootla
48
49 125 Gorge. None of these sections were investigated by Young and Gostin (1991), yet
50
51 126 they yield exceptionally high quality exposure. The sections are ideally situated in a
52
53 127 region subject to only low grade metamorphism during the Early Palaeozoic
54
55 128 Delamerian Orogeny (Preiss, 1987), whereas mid-amphibolite facies affect correlative
56
57
58
59
60

1
2
3 129 sediments in the Adelaide region. Our objectives are (1) to highlight a clear
4
5 130 glaciogenic source for the Bolla Bollana Formation, (2) to reject a rift-only origin for
6
7 131 diamictites, and (3) to present a new depositional model for the sequence as a trough-
8
9 132 mouth fan succession.
10

11
12 133

13
14 134 **FACIES ANALYSIS**

15
16 135 The thickness of the Yudnamutana Subgroup in the North Flinders Basin is estimated
17
18 136 to reach 6000 m in the Yudnamutana Trough (Young and Gostin, 1991),
19
20 137 approximately 30 km NW of the study area. Herein, we focus on exceptionally well-
21
22 138 preserved, high quality sections rather than attempting a complete stratigraphic
23
24 139 traverse. Each of the three facies associations described and interpreted below occur
25
26 140 in multiple locations in the Arkaroola district. We recognise a diamictite facies
27
28 141 association, a channel belt facies association, and a sheet heterolithics facies
29
30 142 association. Below, data from three detailed logged sections are presented (**Fig. 4**).
31
32
33
34 143

35
36 144 **Diamictite facies association**

37
38 145

39
40 146 *Description*

41
42
43 147 This facies association is highly heterogeneous and in terms of volume dominates the
44
45 148 Bolla Bollana Formation (**Fig. 5 A**). Uninterrupted accumulations >90 m thick are
46
47 149 common (e.g. Tillite Gorge: **Fig. 4 B**; **Fig. 5 A**). Diamictites are sandy throughout,
48
49 150 including both clast-poor and clast-rich varieties (*sensu* Moncrieff, 1989), with pebble
50
51 151 to predominantly boulder sized clasts. Bed thickness varies considerably between 1-
52
53 152 15 m (thus reaching megabed dimensions *sensu* Marjanac, 1996) (**Fig. 5 B**). With
54
55
56
57
58
59
60

1
2
3 153 some exceptions, most bed contacts are parallel to one another with minimal evidence
4
5 154 for erosive contacts.
6

7 155

8
9
10 156 Both massive and well stratified diamictites occur as end-members of a
11
12 157 continuum; most beds exhibit at least some diffuse stratification. In some cases,
13
14 158 pronounced variations in clast content (20-60%) occur in successive beds (e.g. **Fig. 4**
15
16 159 **A**, 15-25 m; **Fig. 5 C**). In thick beds, upward transitions from stratified through
17
18 160 massive facies occur, accompanied by an increase in clast size and content (**Fig. 4 B**,
19
20 161 43-73 m). In stratified clast-poor diamictites, isolated clasts of pebble to boulder size
21
22 162 downwarp and pierce underlying laminations; overlying laminae are unaffected (**Fig.**
23
24 163 **5 D**). Sand lenses, or lens-shaped clast-free zones in the diamictite, occur both at the
25
26 164 bottom and top of some beds. Throughout the facies association, clasts are typically
27
28 165 equant, and sub-rounded to sub-angular. The base of the thickest observed bed in the
29
30 166 Tillite Gorge section (**Fig. 4 B**, 43 m) shows a highly undulose contact(**Fig. 5 E**).
31
32 167 Clasts with polished surfaces and crosscutting striations locally occur (**Fig. 5 F**).
33
34 168

35
36
37
38 169 *Interpretation*

39
40 170 The diamictite facies association is interpreted largely as a suite of glaciogenic debris
41
42 171 flows (GDFs) deposited in a subaqueous setting. The organisation of the diamictites
43
44 172 into clearly defined beds indicates repeated emplacement of flows. The typical
45
46 173 absence of erosive contacts is attributed to hydroplaning at the head of the flow,
47
48 174 thereby lubricating the base of the flow and protecting the underlying bed from
49
50 175 cannibalisation (e.g. Laberg and Vorren, 2000). The upsection increase in clast
51
52 176 abundance and size is consistent with kinetic sieving within the flow, to generate
53
54 177 inverse grading (Talling *et al.*, 2012). The downwarping of laminae beneath pebbles
55
56
57
58
59
60

178 in the stratified clast-poor diamictites (**Fig. 5 D**) are interpreted as impact structures
179 produced by falling dropstones. Whilst clasts sinking into water saturated sediment
180 can produce dropstone-like texture in a debris flow, such clasts typically behave
181 similarly to tectonic augen, with concomitant shearing of adjacent laminae as the flow
182 evolves (Hart and Roberts, 1994). Thus, in addition to downslope mass flow, evidence
183 for subaqueous sedimentation and ice-rafted debris accumulation is preserved. Given
184 the compositional similarity of strata both below and above the undulose bed contacts,
185 (**Fig. 5 E**) it is likely that this feature developed through differential compaction rather
186 than through erosion. The presence of clasts with crosscutting striations (**Fig. 5 F**)
187 strongly supports glacial derivation. Specifically, the crosscutting striations indicate
188 rotation of the clasts, either in basal ice, at the ice-bed interface, or within the
189 deforming bed beneath an ice mass (Benn and Evans, 2010, p. 361). The exceptional
190 preservation of striations supports incorporation into the GDFs via ice-rafting, thereby
191 protecting clast surfaces from the erosion processes anticipated during downslope re-
192 mobilisation.

194 **Channel belt facies association**

196 *Description*

197 A variety of scour and fill structures, measuring 5-14 m wide, and 2-3.5 m depth, are
198 a key feature of this facies association (**Fig. 4 B**, 95-113 m; **Fig. 6 A, B**). The scours
199 crosscut, with multiple generations apparent over a few metres (**Fig. 6 A, B**).
200 Lithologies include pebble to granule conglomerates, sandstones and siltstones,
201 together with subordinate sandy diamictites. Some of the scours are mud-filled and re-
202 incised by an overlying channel (**Fig. 6 C**). The base of most beds is irregular (**Fig. 6**

203 D). Normally-graded bedding is typical, with transitions from granule conglomerate
204 through planar-bedded sandstone well expressed in Tillite Gorge as R1 through S3
205 turbidite divisions of Lowe (1982) (e.g. **Fig. 4 B**, 99-103 m; **Fig. 7A**). Soft-sediment
206 deformation structures in sandstone include recumbent folds (**Fig. 7 B**), curvilinear
207 grooves on the upper surfaces of sandstone beds (**Fig. 7 C**) and flame structures. This
208 suite of deformation structures is concentrated at a discrete stratigraphic interval
209 (“shear zone” at 25 m, log B, Fig. 4). Sandy diamictites form sheet-like beds of 0.3-1
210 m, and contain sub-rounded to rounded clasts with striated faces (**Fig. 7 D**).
211 Siltstones occur both within channel structures, and as sheet-like lithosomes traceable
212 for several tens of metres. In both cases, siltstones are poorly stratified, yet bear rare
213 clasts of pebble to boulder size; these pierce and downwarp underlying laminations,
214 with overlying laminations unaffected (**Fig. 7 E, F**).

215

216 *Interpretation*

217 The scour and fill structures are interpreted as channels cut by turbidity currents and
218 filled with turbidites. The coarse calibre of some of the channel fills, and the
219 characteristic R1 through S3 turbidite motif (Lowe, 1982), implies a relatively
220 proximal location on the fan (Reading and Richards, 1994). The particularly coarse-
221 calibre (gravelly) material at the base of some channels is suggestive of a lag deposit
222 (Alpak et al., 2013). By comparison, the finer-grained channel fills are interpreted to
223 record lower energy deposition in either a slightly more distal location on the fan or
224 alternatively a finer-grained sediment source. Specifically, silt-plugged channels may
225 suggest that the channels are filled by low density turbidites (Talling et al., 2012).
226 These deposits represent off-axis / channel margin facies (Camacho *et al.*, 2002) or
227 coarse-grained sediment bypass (Talling et al., 2012), and probably record deposition

228 of these turbidites more distal to the sediment source than their coarser-grained
229 counterparts.

230
231 The suite of soft-sediment deformation structures is compatible with rapid
232 subaqueous deposition: recumbent folds can be indicative of gravitational instability
233 and downslope slumping (Maltman, 1994), whereas flame structures are probably
234 examples of Rayleigh-Taylor instabilities generated at a grain-size / bed interface
235 (Allen, 1984; Collinson and Thompson, 1987). Numerical modelling of flame
236 structures indicates that their genesis is promoted when relatively low viscosity,
237 Newtonian fluids (the sand layer) rest on underlying clays (Harrison and Maltman,
238 2003). These conditions may be satisfied by rapid sedimentation or liquefaction. The
239 curvilinear grooves on the upper surface of beds are interpreted as intra-bed slip
240 planes, akin to hydroplastic slickensides (Petit and Laville, 1987) produced by the
241 shearing of soft sediment in response to downslope movement. Shanmugam *et al.*
242 (1995) described similar features from the Cretaceous and Palaeogene of the North
243 Sea. A later tectonic origin can be dismissed on account of their local occurrence,
244 curvilinear geometry, absence of asperities, and lack of mineralisation (c.f. Petit and
245 Laville, 1987).

246
247 The presence of “impact structures” (curvature, deflection and puncturing of
248 underlying laminations: Bennett *et al.*, 1996) beneath limestones clearly points to ice-
249 rafted debris (IRD) (e.g. Eyles *et al.*, 2007). Moreover, the presence of polished and
250 striated clast surfaces also indicates a clear glacial derivation. Despite the absence of
251 impact structures in the sheet-like siltstones, the presence of limestones may likewise
252 indicate rafting from icebergs, or alternatively sub-ice shelf deposition (Benn and

Evans, 2010). By analogy to comparable facies in the diamictite facies association, the diamictites in the channel belt facies association are also interpreted as the product of glaciogenic debris flows.

256

257 **Sheet heterolithics facies association**

258

259 *Description*

These deposits include a heterogeneous collection of lithologies ranging from granule conglomerates and diamictites, sandstones, siltstones, shales and dolostones. At outcrop, these lithologies are well differentiated, forming tabular beds that can be traced for tens to hundreds of metres along strike. Decimetre to metre-scale fining upward cycles is typical, with well-expressed examples in Weetootla Gorge (**Fig. 4 C**, 23-75 m; **Fig. 8 A**). Fining upward cycles commence with sharp-based and locally scoured surfaces, overlain by granule-lags or massive sandstones (**Fig. 8 B**), becoming parallel laminated upsection. Supercritical climbing ripple cross-laminated sandstones and siltstones (**Fig. 8 C**) are typical in the upper part of many fining upward cycles (e.g. 56 m, 68 m, 85 m, 100 m at Weetootla Gorge: **Fig. 4 C**). The crests of the ripple-cross laminae show an aggradational to weakly progradational character (**Fig. 8 C**). Rarely, the fining upward intervals are interrupted by clast-poor, sandy diamictites which do not exceed 1 m in thickness (**Fig. 8 D**). Siltstone and shale occur at the top of the fining upward cycles (**Fig. 8 E**). Lonestones with impact structures occur in most facies, including the cross-laminated sandstone (e.g. 102 m, Tillite Gorge: **Fig. 4 B**; **Fig. 8 B**, arrowed clast) and in shale beds (**Fig. 8 E**). The metre-scale fining upward cycles are themselves organised into multi-metre thick coarsening and fining upward motifs. At three intervals (25 m, 37 m, 66.5 m at

278 Weetootla Gorge: **Fig. 4 C**) we observed buff coloured, delicately parallel laminated,
279 mud-grade dolostones (**Fig. 8 F**).

281 *Interpretation*

282 This facies association is interpreted to represent deposition in an inter-channel part of
283 a subaqueous fan system, where the well-expressed, metre-scale fining upward cycles
284 are interpreted to record repeated emplacement of turbidity flows. A basal scour and
285 lag, succeeded by a massive then parallel laminated sandstone interval, succeeded by
286 climbing ripple cross-lamination, is a motif common to all models of turbidite genesis
287 (c.f. Bouma, 1962; Lowe, 1982; Mutti, 1996; Talling *et al.*, 2012). Whilst the tabular
288 geometry of the cycles is compatible with deposition as high-density turbidites (i.e.
289 divisions T_A, T_{B-2} and T_{B-3} in the modified Bouma nomenclature: Talling *et al.*, 2012)
290 The occurrence of lonestones with impact structures, interpreted as dropstones, in
291 ripple cross-laminated siltstones is strong evidence for glacial influence. The
292 supercritical styles of ripple cross-lamination testify to high rates of sediment
293 delivery, and tractive velocities of $<0.6 \text{ m s}^{-1} \text{ m}$ (e.g. Bridge and Demicco, 2008). The
294 occurrence of large clasts within these facies is at odds with the low velocities
295 required for the formation of ripple cross-lamination, which are thus interpreted as
296 ice-rafted debris. Furthermore, turbidity flows typically demonstrate low yield
297 strength and cannot support clasts through buoyancy within the flow (Shanmugam,
298 2002). Although Lowe (1982) suggested that sand-dominated traction carpets in dense
299 sandy turbidites were capable of periodically bouncing clasts as suspension load,
300 these inferred processes have not been observed in turbidity currents (Talling *et al.*,
301 2012). The co-occurrence of thin sandy diamictites, interpreted as the dilute distal

fronts of glaciogenic debris flows, strengthens the interpretation of a glacial influence on sedimentation.

The organisation of the Bouma cycles into both coarsening and fining upward motifs at the multi-metre scale is respectively suggested to record the buildout and abandonment of subaqueous fan lobes, in a similar manner to other glacially sourced subaqueous fan systems (Le Heron et al., 2008). The delicately laminated dolostones at the top of some fining-upward cycles remains cryptic. They do not occur in finer-grained, turbidite-dominated systems of the central Flinders Ranges (e.g. Busfield and Le Heron, in review; Le Heron et al., 2011), which likely indicates that the dolostones are of local significance. They are presently suggested to record chemical or biological precipitation during or following lobe abandonment, although the precise mechanisms of precipitation requires further study. Their lonestone-free textures merit one further consideration, however. If subaqueous sedimentation rates of IRD were similar everywhere on the fan system at a given time, comparable deposits should form simulatenously. Given the absence of lonestones in the dolostones, intervals of IRD-free conditions might be proposed, thus suggesting that these might be associated with lower rates of deposition and therefore no floating ice.

STACKING PATTERNS

The vertical stacking motif of facies associations is an important consideration in a glacially-sourced sedimentary system and may allow the dynamics of former ice sheets to be elucidated. At Stubb's Waterhole, the diamictite facies association predominates but those strata are intercalated with ~5 m thick developments of the

327 sheet heterolithics facies association. A considerably thicker example of that facies
328 association is found interbedded with the diamictite facies association at Weetootla
329 Gorge (23- 75 m: **Fig. 4 C**). Given the differences in thickness at both localities, it is
330 proposed that the Stubb's Waterhole occurrence may represent the margins of a
331 turbidite lobe system (e.g. Pr  lat et al., 2010), whereas the Weetootla Gorge examples
332 are more compatible with the core of a turbidite lobe system. Note, however, that our
333 data do not represent a complete traverse through the formation in either case.
334 Interstratification of the diamictite facies association and the channel belt facies
335 association, at the tens of metres scale at Tillite Gorge testifies to the likely
336 synchronous co-development of turbidite channel belts and GDF deposits. This
337 implies that each sub-environment, recognised in the form of the three facies
338 associations, co-existed during deposition of the Bolla Bollana Formation.

340 In the Arkaroola area, the Bolla Bollana Formation maps as a continuous
341 stratigraphic unit around the north-eastern extremity of the Gammon Ranges. Preiss *et*
342 *al.* (1993, 1998, 2000, 2011), interpret the North Flinders Basin as a region that
343 experienced extension synchronous with glaciation by Sturtian ice sheets. Progressive
344 thickness increases to the north are explained by the development of en echelon half
345 graben (Preiss et al., 2011). Crustal extension, during the fragmentation of Rodinia,
346 which accounted for the generation of substantive accommodation space, was also
347 considered to be important by Young and Gostin (1988, 1989, 1990, 1991). However,
348 the location of many of these faults remains unclear: the 1:250,000 sheet (Copley:
349 Coats, 1973) reveals no faults specifically causing abrupt thickness changes in the
350 Bolla Bollana Formation.

We argue that the substantial thickness and sedimentary architecture of the Bolla Bollana Formation can be explained by ice sheet dynamics alone. The diamictite facies association records glaciogenic debris flows (GDFs) with secondary ice-rafting in the proximal part of a subaqueous basin (**Fig. 9**). The presence of faceted, polished and striated clasts in the Bolla Bollana Formation strongly implies direct glacial derivation. This is because cannibalised or reworked (second generation) debris flows tend to erode and smooth clast surfaces (Le Heron *et al.*, 2013). The glaciogenic debris flows likely became diluted basinward, developing into turbulent underflows, which built up a series of lobes and channel belts (i.e. channel belt facies association) on a large subaqueous fan (**Fig. 9**). The sheet heterolithics facies association represents lobe deposits (e.g. Pr  lat *et al.*, 2010) in the inter-channel part of a subaqueous fan system. These lobes were influenced by local ice rafting as a secondary sediment source (**Fig. 9**). Abandonment of the lobes locally resulted in some highly unusual laminated dolostone deposits. These superficially resemble “cap dolostone” deposits (e.g. Rose and Maloof, 2010). As noted earlier, given their probable stratigraphic context as lobe abandonment facies it is unlikely that they have any wider significance. The lack of evidence for IRD in these specific facies- a texture which might be expected to appear more prominently once sediment supply is arrested- is also puzzling.

371

372

373 A NEOPROTEROZOIC TROUGH-MOUTH FAN?

374 It is suggested that the Bolla Bollana Formation is a trough mouth fan (TMF) (**Fig. 9**)
375 deposited seaward of a comparatively small palaeo-ice stream. This interpretation is
376 fully consistent with 1) clear evidence for glacial processes in every facies association

1
2
3
4
5
6
7
8
9
10
11
12
13
14
15
16
17
18
19
20
21
22
23
24
25
26
27
28
29
30
31
32
33
34
35
36
37
38
39
40
41
42
43
44
45
46
47
48
49
50
51
52
53
54
55
56
57
58
59
60

377 of the Bolla Bollana Formation, 2) the substantial thickness of the succession which
378 compares closely to stacked mass flow deposits of the Bear Island Fan (Taylor *et al.*,
379 2002; Ó Cofaigh *et al.*, 2003), and 3) the stratigraphic motif and nature of the facies
380 associations preserved.

381

382 Evidence for glaciation throughout the Bolla Bollana Formation is pervasive
383 and includes dropstone textures (in turbidites, as well as hemipelagic muds), together
384 with faceted, polished and striated clasts throughout the succession. Boreholes sunk
385 in the Uummannaq Fan (western Greenland) illustrate 300 m thick successions of
386 diamicton that are sharply overlain by mud (Ó Cofaigh *et al.*, 2012). These are closely
387 comparable to stacked examples of the diamictite facies association in Tillite Gorge.
388 Intercalated debrites, turbidites, and ice-rafted debris commonly occur together in
389 depositional models of Pleistocene TMFs (Ó Cofaigh *et al.*, 2012).

390

391 In both the northern and southern hemispheres, trough mouth fans (TMFs)
392 were deposited during Pleistocene glaciations and consist of thick accumulations of
393 glaciogenic detritus (Escutia *et al.*, 2000; Taylor *et al.*, 2002). In this process, fast-
394 flowing ice streams excavate the subglacial substrate and deposit diamictite at the ice
395 front, perched landward of the slope break. In Pleistocene examples, rapid
396 sedimentation of water saturated tills led to unstable slope angles and hence
397 intermittent failure (Dowdeswell *et al.*, 2002). This in turn led to the generation of
398 GDFs derived from collapsing tills (Taylor *et al.*, 2002). In the southern hemisphere,
399 the Wilkes Land continental margin was fed by stacked GDFs, which evolved
400 downslope into turbidites, building up a multi-kilometre thick pile of channelized
401 proglacial detritus (Escutia *et al.*, 2000).

402

403 Regional mapping (Coats, 1973) shows that the Bolla Bollana Formation

404 crops out over at least 1800 km². Assuming a conservative thickness of 1 km in the

405 Arkaroola district, the Bolla Bollana Formation represents approximately 1800 km³ of

406 glaciogenic sediment: impressive, yet substantially less volumetric than the modern

407 Bear Island Fan (ca. 340,000 km³) (Dowdeswell *et al.*, 2002 and refs therein). Part of

408 the reason for this comparatively small volume may lie in the partitioning of the basin

409 by syn-depositional faults (Preiss *et al.*, 2011). From both stratigraphic and facies

410 perspectives, there is good reason to view the North Flinders Basin as a sub-basin

411 disconnected from the central Flinders Ranges further to the south (Preiss *et al.*,

412 2011). Differences between Pleistocene TMF models and our interpretation (**Fig. 9**)

413 include the absence of bioturbation and a lower volume of mud in the Bolla Bollana

414 TMF deposit (c.f. Ó Cofaigh *et al.*, 2002; 2003; 2012). In subaqueous fans, increase in

415 mud content improves the run-out efficiency of turbidites and increases fan size

416 (Reading and Richards, 1994). Another obvious difference is the presence of

417 dolostones in the Bolla Bolla Formation: such dolostones are absent in Pleistocene

418 TMFs. They are, however, almost ubiquitous in the Cryogenian record, typically

419 occurring immediately above the diamictite successions as cap carbonates (e.g.

420 Shields, 2005)..

421

422 The gentle regional dip of the Bolla Bollana Formation (**Fig. 5 A**) precludes

423 mapping of individual debrite megabeds, yet Quaternary analogues may allow some

424 insight into possible maximum lateral dimensions. Debrites on the Bear Island Fan are

425 elongate lobes with individual run-out distances of > 40 km (Laberg and Vorren,

426 2000; Ó Cofaigh *et al.*, 2003). They commence at ~1 km below sea level, extending

1
2
3
4
5
6
7
8
9
10
11
12
13
14
15
16
17
18
19
20
21
22
23
24
25
26
27
28
29
30
31
32
33
34
35
36
37
38
39
40
41
42
43
44
45
46
47
48
49
50
51
52
53
54
55
56
57
58
59
60

427 to approximately 2.5 km depth. The up-dip termination of the debrite lobes
428 approximates the palaeo-ice margin (**Fig. 9**). In addition to the generation of GDFs,
429 the accumulation of thick piles of detritus on trough-mouth fans lends them prone to
430 gravitational collapse (Dowdeswell *et al.*, 2002). Thus, many of the extensional faults
431 and graben structures in the NFB may represent seaward partial collapse of the fan.

432
433 Young and Gostin (1989) provided detailed descriptions and interpretations of
434 comparable successions further north, in the Yudnamutana homestead and surrounds.
435 There, a subaqueous fan system, dominated by boulder-bearing debrites with
436 subordinate turbidites, was envisaged (Young and Gostin, 1989). This interpretation is
437 fully compatible with our own and underscores that an identical range of sub-
438 environments are recognised around the Bolla Bollana outcrop belt (**Fig. 9**). It is clear
439 that the Bolla Bollana Formation contains excellent evidence for glacial sedimentary
440 processes, reinforcing the original work of Mawson (1941, 1949), and making it
441 difficult to argue for a rift-source alone as has been suggested for similar
442 Neoproterozoic diamictite successions (e.g. Eyles and Januszczak, 2004).

443
444 The connection between the Bolla Bollana depocentre and other sub-basins in
445 the central Flinders Ranges is obscure. Rifting is an attractive mechanism to account
446 for the different stratigraphic units preserved in the North Flinders Basin and
447 depocentres further south such as Baratta and Holowilena (Preiss, 2000). It should be
448 stressed, however, that not all sub-basins in the Flinders Ranges preserve clear
449 evidence for rifting. The Holowilena succession, for example, contains delicately
450 interbedded siltstones, diamictites, sandstones, and IRD-bearing shale (Busfield and
451 Le Heron, in review; Le Heron, 2012). Internally, that succession contains

1
2
3 452 disconformities and not angular relationships between bedsets (Le Heron, 2012)
4
5 453 which might be expected where undeformed sediments onlap rotated hangingwall
6
7 454 strata. Nonetheless, correlative successions at Oladdie Creek and Hillpara Creek, in
8
9 455 the central Flinders Ranges, reveal dramatic thickness changes along strike. These
10
11 456 testify to an irregular underlying palaeotopography, which is likely attributed to the
12
13 457 combined influence of pre- and early syn-depositional rift activity and subglacial
14
15 458 downcutting (Busfield and Le Heron, in review).
16
17
18
19 459
20
21 460

22
23 461 The Bolla Bollana Formation provides a unique window into the sedimentary
24
25 462 architecture of a trough-mouth fan (TMF). The interpretation of a TMF is doubly
26
27 463 significant. Firstly, the authors are not aware of any previously described TMFs of
28
29 464 pre-Pleistocene age, and thus the first documentation is provided herein. Secondly, the
30
31 465 Bolla Bollana is the only known outcrop example thus far described of such a fan. It
32
33 466 is probably the case that the generally large scale of these fans (O'Cofaigh, 2012) has
34
35 467 precluded their outcrop-scale interpretation in ancient strata. Whilst volumetrically
36
37 468 less significant in the fan systems than GDFs, the Bolla Bollana succession also
38
39 469 reveals the common occurrence of turbidite intervals, amplifying the importance of
40
41 470 turbidity currents in TMF models (Escutia *et al.*, 2000). The occurrence of correlative
42
43 471 turbidite and debrite-dominated successions is also well reported from subsurface
44
45 472 boreholes elsewhere in southern and central Australia (e.g. Blinman 2 borehole,
46
47 473 central Flinders Ranges; Nicholson 2 borehole, ca. 500 km NW of Arkaroola; Vines 1
48
49 474 borehole, Officer Basin) (Eyles *et al.*, 2007). A clear, glacial influence is reported
50
51 475 from those sections on account of striated and outsized clasts in laminated facies
52
53 476 (Eyles *et al.*, 2007), although it remains unclear how these underflow-dominated
54
55
56
57
58
59
60

477 successions relate laterally to one another. In light of our interpretations, it is possible
478 that these deposits represent an amalgam of overlapping TMFs, line-sourced detritus,
479 or somewhat more disconnected fan systems.

481 In the context of a Neoproterozoic snowball Earth model, Hoffman (2005)
482 argued that palaeo-ice streaming- which he inferred on the basis of irregular
483 topography within the Ghaub glacial succession of Namibia, and the occurrence of a
484 large wedge of grainstone sediment- was “not incompatible with a frozen ocean”.
485 Etienne *et al.* (2007) and Allen and Etienne (2008), meanwhile, pointed out that the
486 highly dynamic nature of tidewater ice sheets directly challenged this view. In
487 particular, the issue of resupply of snow in the accumulation zone of ablating ice
488 sheets- given the presumed arrested hydrological cycle- remains problematic.

490 Some 120 km to the south of Arkaroola, exceptionally exposed, age equivalent
491 successions at Holowilena, Oladdie and Hillpara Creeks, in the central Flinders
492 Ranges (Busfield and Le Heron, in review; Le Heron *et al.* 2011) reveal a highly
493 comparable stratigraphic subdivision in a series of tectonically partitioned basins.
494 These sections identify a clear non-glacial interval within the Wilyerpa Formation,
495 which yields spectacularly preserved hummocky cross strata (HCS), indicative of
496 sea-ice free conditions (Le Heron *et al.*, 2011), followed by a glacial re-advance.
497 Young and Gostin (1991) likewise identified a second major re-advance in the
498 Sturtian, represented by accumulation of the Bolla Bollana Formation. These
499 considerations suggest the Bolla Bollana Formation may correlate with the re-advance
500 succession in the central and southern Flinders Ranges and, if so, suggests deposition
501 of the TMF at Arkaroola in seas which were at least periodically unfrozen.

1
2
3 502
4

5 503 **CONCLUSIONS**
6

7 504 The Bolla Bollana Formation is a spectacularly exposed glaciogenic succession of
8
9 505 Sturtian age in the Arkaroola district. This formation was first investigated by
10
11 506 Mawson (1941, 1949) but subsequently little work has been undertaken at the Tillite
12
13 507 Gorge, Stubb's Waterhole or Weetootla Gorge locations. Detailed sedimentary
14
15 508 logging at these locations, therefore, allows a detailed sedimentary model to be
16
17 509 developed as follows:
18
19

- 20
21 510 • Three facies associations are recognised in the Bolla Bollana Formation.
22
23 511 These are a diamictite facies association (glaciogenic debris flows with
24
25 512 subordinate ice-rafted debris), a channel belt facies association (channelized
26
27 513 turbidites with subordinate IRD) and a sheet heterolithics facies association
28
29 514 (non-channelised turbidites and subordinate IRD). A strong glacial influence
30
31 515 on sedimentation is inferred, reinforcing previous interpretations of Young and
32
33 516 Gostin (1991). A rift-related source for the diamictites is rejected.
34
35
36 517 • A depositional model based on detailed observations and interpretations from
37
38 518 all three facies associations proposes that the Bolla Bollana Formation was
39
40 519 deposited as a trough-mouth fan, seaward of the terminus of a small ice
41
42 520 stream. Rapid ice flux promoted high erosion rates and sediment delivery. At
43
44 521 the ice margin, GDF deposited multi-storey stacks of diamictite, many
45
46 522 deposited as megabeds. Slope failure and / or dilution of these flows
47
48 523 basinward ignited turbidites, which cut channel geometries onto the proximal
49
50 524 and medial parts of the fan. Non-channelised turbidites demonstrate well
51
52 525 organised multi-metre coarsening and fining upward motifs, interpreted to
53
54 526 record build out and abandonment of fan lobes. Laminated dolostones are an
55
56
57
58
59
60

unusual fan-lobe abandonment facies and bear superficial resemblance to post-glacial “cap dolostones” elsewhere.

- Previous models of tectonic compartmentalisation a result of rifting post- 750 Ma (e.g. Preiss, 2000; Young and Gostin, 1991; Eyles and Januszczak, 2004) may help in explaining dramatic regional differences in facies and internal Sturtian stratigraphy. In the Bolla Bollana Formation, however, it is suggested that a tectonic mechanism is not required by reference to Cenozoic trough-mouth fan systems where substantive diamictite accumulations occur.

ACKNOWLEDGMENTS

The authors wish to thank Doug Sprigg for sharing with us his knowledge of the pioneer’s experiences in the Arkaroola area, for permission to work in the area, and general helpfulness. We are very grateful to two anonymous referees whose comments significantly improved the manuscript. We also want to thank Professor Nick Eyles for additional comments which helped improve the final version of the paper, and Professor Stephen Rice, the handling editor, for assistance and carefully considered input. This work was funded by a National Geographic Explorer Fund grant to DPLeH.

Figure captions

Figure 1: Geological sketch map of the Arkaroola region (modified and simplified after Coats, 1973). Note the location of the Tillite Gorge, Stubb’s Waterhole and Weetootla Gorge sections which are shown on figure 4.

Figure 2: Northern Flinders Basin map, reproduced from Young and Gostin (1991). The palaeocurrent data, shown here schematically, derive from a variety of sources (flute casts, ripple cross laminae) and have been used to infer the development of syn-glacial horst and graben topography (Young and Gostin, 1991). The outline of various sub-basins are shown with a solid line, with stippling marking the internal margins of these sub-basins.

Figure 3: Stratigraphy of the Neoproterozoic of the Arkaroola area, with subdivisions of the Sturt glacial succession based on Young and Gostin (1989). The internal lithostratigraphy of the Sturt glacial succession varies dramatically even over the comparatively small region of the northern Flinders Ranges (c.f. Young and Gostin, 1988, 1989, 1990, 1991). In the Arkaroola district, a threefold division is recognised with the Fitton Formation at the base, the Bolla Bollana Formation in the middle, and the Lyndhurst Formation as the uppermost unit within the Yudnamutana Subgroup. This paper specifically examines the Bolla Bollana Formation.

Figure 4: Detailed sedimentary logs through the Bolla Bollana Formation in the Arkaroola district (see Fig. 1 for location of sections). Each is a partial section through the exposure at each locality rather than a complete section. A: Stubb's Waterhole. B: Tillite Gorge. C: Weetootla Gorge. Note that in the case of the diamictites, the grain size in each of the logs refers to grain size of the matrix: maximum clast size, where possible was also measured. These latter data are shown to the right of the logs.

Figure 5: Representative photographs of facies within the diamictite facies association. A: Outcrop perspective of the Tillite Gorge locality, showing thickly bedded diamictites dipping toward the right of the photograph. B: Base of a diamictite megabed (42-67 m, Fig. 4 B) with geologist for scale. C: Clast-poor diamictite overlain by clast-rich diamictite, with geological hammer for scale placed at the boundary. D: Impact structure beneath gneiss pebble in well-stratified diamictite. Rounded clasts are quite typical. E: Undulose contact at the base of a diamictite megabed. Note that this undulose character probably records differential compaction. Scale bar: 1 m. F: Face of a polished and striated sandstone boulder, showing crosscutting striation orientations.

Figure 6: A and B: Panoramic photo and corresponding sketch of stacked channel geometries in the channel belt facies association. Note also the downlapping strata of the diamictite facies association directly above. C: Low angle channel incision cutting down towards the left of the photograph (marked by solid white line), clearly truncating recessive siltstones, themselves infilling a channel scour. D: Low amplitude scour at the base of a sandstone bed: evidence for erosion-based beds even where clear channel geometries are not observed.

Figure 7: A: Typical fining upward sequence, interpreted as a turbidite bed. In this example, pebble to cobble-grade clasts beneath the hammer pass upward over 10 cm into granular conglomerates, and finally well differentiated, moderately to well-sorted sandstone above the hammer handle. B: Recumbent fold in a turbidite. C: Curvilinear grooves on a sandstone surface, interpreted to record intrastratal shear in sandstones. The absence of asperities or quartz/ calcite mineralisation discounts a tectonic origin. D: Striated lonestone within siltstone: a putative dropstone emplaced toward the top of a Bouma sequence. E and F: Two examples of dropstones with clear impact structures in laminated siltstone intervals.

Figure 8: Representative photographs of facies within the sheet heterolithics facies association. A: Repetitively stacked, decimetric Bouma cycles. Note coin for scale. B: Lonestones to the left of the coin within fine-grained, climbing ripple cross-laminated sandstone. C: Detail of photo B showing prograding crest (from right to left) of a

609 climbing ripple. Note that tractive velocities predicted within the field of ripple
610 formation (e.g. Bridge and Demicco, 2008) are insufficient to transport pebble-sized
611 clasts. Thus, a dropstone origin is deduced. D: Lonestone with deflected laminations
612 above the clast: possibly as a result of compaction. Field of view 7 cm. E: Quartzite
613 dropstone, with impact structure (truncation and piercing of shale laminae) beneath
614 the coin. Laminated dolostone (25 m, Fig. 4 C).

615
616 *Figure 9: Simple depositional model for the Bolla Bollana Formation. We interpret a*
617 *glaciomarine basin, a general setting consistent with previous work (e.g. Coats, 1981;*
618 *Young and Gostin, 1989, 1991). Glaciogenic debris flows fed the basin, evolving into*
619 *turbidites down depositional dip. Channel belts and inter-channel areas recording*
620 *slightly finer grained turbidites are recognised. Phases of fan-lobe buildout and*
621 *abandonment are recognised, with these processes likely a result of autocyclic*
622 *switching of channel belts and sediment supply rather than basin-scale ice dynamics.*
623 *The scale of the sedimentary system, and clear evidence for a strong glacial influence*
624 *on sedimentation in all facies associations, suggests that the Bolla Bollana deposit is a*
625 *trough-mouth fan deposit, with huge volumes of glaciogenic debris supplied to a*
626 *subaqueous setting. This is the first such interpretation from the Neoproterozoic*
627 *record.*

628
629

630

631 **REFERENCES**

632 **Allen, J.R.L.** (1984) *Sedimentary Structures: Their Character and Physical Basis,*
633 *volumes I and II. Elsevier, Amsterdam.*

634

635 **Allen, P.A. and Etienne, J.L.** (2008) *Sedimentary Challenge to Snowball Earth:*
636 *Nature Geoscience, 1, p. 817-825.*

637

638 **Alpak, F., Barton, M.D. and Naruk, S.J.** (2013) The impact of fine-scale turbidite
639 channel architecture on deep-water reservoir performance. *AAPG Bulletin*, **97**, 251-
640 284.

641

642 **Arnaud, E.** (2012) The paleoclimatic significance of deformation structures in
643 Neoproterozoic successions. *Sedimentary Geology*, **243-244**, 33-56.

644

645 **Bennett, M.R.** (2003) Ice streams as the arteries of an ice sheet: their mechanics,
646 stability and significance. *Earth-Science Reviews*, **61**, 309–339.

647

648 **Bouma, A.H.** (1963) Sedimentary facies model of turbidites. *AAPG Bulletin*, **47** (2),
649 351.

650

651 **Bridge, J.S. and Demicco, R.V.** (2008) *Earth Surface Processes, Landforms and*
652 *Sediment Deposits. Cambridge University Press, UK, 815p.*

653

654 **Busfield, M.E. and Le Heron, D.P.** (in press) Glacitectonic deformation in the Chuos
655 Formation of northern Namibia: implications for Neoproterozoic ice dynamics.
656 *Proceedings of the Geologist's Association.* doi: /10.1016/j.pgeola.2012.10.005

657

- Busfield, M.E. and Le Heron, D.P.** (in review) Glaciodynamic signature of a Sturtian ice sheet in the Flinders Ranges, South Australia. *Journal of Sedimentary Research*.
- Coats, R.P.** (1973) Copley, South Australia. Explanatory Notes. 1:250,000 Geological Series, Sheet SH/54-9. Geological Survey of South Australia, 38 pp.
- Coats, R.P.** (1981) Late Proterozoic (Adelaidian) tillites of the Adelaide Geosyncline, in: Hambrey, M.J., Harland, W.B. (Eds.), *Earth's Pre-Pleistocene Glacial Record*: Cambridge, Cambridge University Press, 537-548.
- Collinson, J.D. and Thompson, D.B.** (1987) *Sedimentary Structures*, 2nd edition. Chapman and Hall, London.
- Corkeron, M.L.** (2007) 'Cap carbonates' and Neoproterozoic glacial successions from the Kimberley region, north-west Australia. *Sedimentology*, **54**, 871-903.
- Daily, B., Gostin, V.A. and Nelson, C.A.** (1973) Tectonic origin for an assumed glacial pavement of Late Proterozoic age, South Australia. *Journal of the Geological Society of Australia*, **20**, 75-78.
- Dowdeswell, J.A., O'Cofaigh, C., Taylor, J., Kenyon, N.H., Mienert, J. and Wilken, M.** (2002) On the architecture of high-latitude continental margins: the influence of ice-sheet and sea-ice processes in the Polar North Atlantic. In: Dowdeswell, J.A. & O'Cofaigh, C. (eds) *Glacier-Influenced Sedimentation on High-Latitude Continental Margins*. Geological Society, London, Special Publications 203, 33-54.
- Escutia, C., Eittreim, S.L., Cooper, A.K. and Nelson, C.H.** (2000) Morphology and acoustic character of the Antarctic Wilkes Land turbidite systems: icesheet- sourced versus river-sourced fans. *Journal of Sedimentary Research*, **70**, 84-93.
- Etienne, J.L., Allen, P.A., Rieu, R. and Le Guerroue, E.** (2007) Neoproterozoic glaciated basins: a critical review of the Snowball Earth hypothesis by comparison with Phanerozoic glaciations, in: Hambrey, M.J., Christoffersen, P., Glasser, N.F., Hubbard, B. (Eds.), *Glacial Processes and Products*. International Association of Sedimentologists, Special Publications, 436 pp.
- Eyles, C.H., Eyles, N. and Grey, K.** (2007) Palaeoclimate implications from deep drilling of Neoproterozoic strata in the Officer Basin and Adelaide Rift Complex of Australia; a marine record of wet-based glaciers. *Palaeogeography, Palaeoclimatology, Palaeoecology*, **248**, 291-312.
- Eyles, N. and Januszczak, N.** (2004) 'Zipper-rift': a tectonic model for Neoproterozoic glaciations during the breakup of Rodinia after 750 Ma. *Earth-Science Reviews*, **65**, 1-73.
- Eyles, N. and Januszczak, N.** (2007) Syntectonic subaqueous mass flows of the Neoproterozoic Otavi Group, Namibia: where is the evidence of global glaciation? *Basin Research*, **19**, 179-198.

708 **Fairchild, I. and Kennedy, M.J.** (2007) Neoproterozoic glaciation in the Earth
709 System. *Journal of the Geological Society of London*, **164**, 895–921.
710

711 **Harrison, P. and Maltman, A.J.** (2003) Numerical modelling of reverse-density
712 structures in soft non-Newtonian sediments. In: van Rensbergen, P., Hillis, R.R.,
713 Maltman, A.J. & Morley, C.K. (eds). Subsurface sediment mobilization. *Geological*
714 *Society, Special Publications*, **216**, 35-50.
715

716 **Hart, J.K. and Roberts, D.H.** (1994) Criteria to distinguish between subglacial
717 glaciotectonic and glaciomarine sedimentation, I. Deformation styles and
718 sedimentology. *Sedimentary Geology*, **91**, 191-213.
719

720 **Hoffman, P.F.** (2005) 28th DeBeers Alex Du Toit Memorial Lecture, 2004. On
721 Cryogenian (Neoproterozoic) ice-sheet dynamics and the limitations of the glacial
722 sedimentary record. *South African Journal of Geology*, **108**, 557-576.
723

724 **Hoffman, P.F. and Schrag, D.P.** (2002) The snowball Earth hypothesis: testing the
725 limits of global change. *Terra Nova*, **14**, 129-155.
726

727 **Hoffman, P.F., Kaufman, A.J., Halverson, G.P. and Schrag, D.P.** (1998) A
728 Neoproterozoic Snowball Earth. *Science*, **281**, 1342-1346.
729

730 **Laberg, J.S. and Vorren, T.O.** (2000) Flow behaviour of the submarine glacial
731 debris flows on the Bear Island Trough Mouth Fan, western Barents Sea.
732 *Sedimentology*, **47**, 1105-1117.
733

734 **Le Heron, D.P.** (2012) The Cryogenian record of glaciation and deglaciation in South
735 Australia. *Sedimentary Geology*, **243-244**, 57-69.
736

737 **Le Heron, D.P., Khoukhi, Y., Paris, F., Ghienne, J.-F., Le Hérissé,** 2008. Black
738 shale, grey shale, fossils and glaciers: anatomy of the Upper Ordovician–Silurian
739 succession in the Tazzeka Massif of eastern Morocco. *Gondwana Research*, **14**,
740 483–496.
741

742 **Le Heron, D.P., Cox, G.M., Trundle, A.E. and Collins, A.** (2011) Sea-ice free
743 conditions during the early Cryogenian (Sturt) glaciation, South Australia. *Geology*,
744 **39**, 31-34.
745

746 **Le Heron, D.P., Busfield, M.E., Kamona, A.F.** (2013). Interglacial on snowball
747 Earth? Dynamic ice behaviour revealed in the Chuos Formation, Namibia.
748 *Sedimentology*, **60**, 411-427.
749

750 **Lowe, D.R.** (1982) Sediment gravity flows: II. Depositional models with special
751 reference to the deposits of high-density turbidity currents. *Journal of Sedimentary*
752 *Petrology*, **52**, 279-297.
753

754 **Macdonald, F.A., Schmitz, M.D., Crowley, J.L., Roots, C.F., Jones, D.S., Maloof,**
755 **A.C., Strauss, J.V., Cohen, P.A., Johnson, D.T. and Schrag, D.P.** (2010b)
756 Calibrating the Cryogenian. *Science*, **327**, 1241-1243.
757

- 758 **Maltman, A.** (1994) The Geological Deformation of Sediments. Chapman and Hall,
759 Cambridge. 384 pp.
- 760
- 761 **Marjanac, T.** (1996). **Deposition of megabeds (megaturbidites) and sea-level**
762 **change in a proximal part of the Eocene-Miocene flysch of central Dalmatia**
763 **(Croatia).** *Geology*, **24**, 543-546.
- 764
- 765 **Mawson, D.** (1941) Middle Proterozoic sediments in the neighbourhood of Copley.
766 *Transactions of the Royal Society of South Australia*, **65**, 304–311.
- 767
- 768 **Mawson, D.** (1949) Sturt tillite of Mount Jacob and Mount Warren Hastings, north
769 Flinders Ranges. *Transactions of the Royal Society of South Australia*, **72**, 244–251.
- 770
- 771 **Moncrieff, A.C.M.** (1989) Classification of poorly-sorted sedimentary rocks.
772 *Sedimentary Geology*, **65**, 191-194.
- 773
- 774 **Mutti, E., Tinterri, R., Remacha, E., Mavilla, N., Angella, S. and Fava, L.** (1999)
775 An introduction to the analysis of ancient turbidite basins from an outcrop
776 perspective. *American Association of Petroleum Geologists, Continuing Education*
777 *Course Notes Series*, **39**. Oklahoma, USA.
- 778
- 779 **Ó Cofaigh, C., Taylor, J., Dowdeswell, J.A., Rosell-Melé, A., Kenyon, N.H.,**
780 **Evams, J. and Mienert, J.** (2002) Sediment reworking on high-latitude continental
781 margins and its implications for palaeoceanographic studies: insights from the
782 Norwegian-Greenland Sea. In: Dowdeswell, J.A. & Ó Cofaigh, C. (Eds) *Glacier-*
783 *Influenced Sedimentation on High-Latitude Continental Margins. Geological*
784 *Society, London, Special Publication*, **203**, 325–348.
- 785
- 786 **Ó Cofaigh C, Taylor J, Dowdeswell J.A. and Pudsey, C.J.** (2003) Palaeo-ice
787 streams, trough mouth fans and high-latitude continental slope sedimentation.
788 *Boreas*, **32**, 37–55.
- 789
- 790 **Ó Cofaigh, C., Andrews, J.T., Jennings, A.E., Dowdeswell, J.A., Hogan, K.A.,**
791 **Kilfeather, A.A. and Sheldon, C.** (2012) Glacimarine lithofacies, provenance and
792 depositional processes on a West Greenland trough-mouth fan. *Journal of*
793 *Quaternary Science*, DOI: 10.1002/jqs.2569.
- 794
- 795 **Petit, J.-P. and Laville, E.** (1987) Morphology and microstructures of hydroplastic
796 slickensides in sandstone. In: Jones, M.E., Preston, R.M.F. (Eds.), *Deformation of*
797 *Sediments and Sedimentary Rocks. Geological Society of London Special*
798 *Publication*, **29**, pp. 107–121.
- 799
- 800 **Preiss, W.V.** (1987) A synthesis of palaeogeographic evolution of the Adelaide
801 Geosyncline. In: Preiss, W.V. (Compiler), *The Adelaide Geosyncline. Late*
802 *Proterozoic Stratigraphy, Sedimentation, Palaeontology and Tectonics. Geol. Surv.*
803 *South Australian Bulletin*, **53**, 315–409.
- 804
- 805 **Preiss, W.V.** (1993) Neoproterozoic. In: Drexel, J.F., Preiss, W.V., Parker, A.J.
806 (Eds.), *The geology of South Australia*, vol. 1, *The Precambrian: South Australia.*
807 *Geological Survey, Bulletin*, **54**, pp. 170–224.

1
2
3
4
5
6
7
8
9
10
11
12
13
14
15
16
17
18
19
20
21
22
23
24
25
26
27
28
29
30
31
32
33
34
35
36
37
38
39
40
41
42
43
44
45
46
47
48
49
50
51
52
53
54
55
56
57
58
59
60

808
809 **Preiss, W.V.** (1999) Parachilna Sheet SH54-13. 1:250 000 scale Geological Map and
810 Explanatory Notes, Primary Industries and Resources South Australia. Second
811 edition. 52p.
812
813 **Preiss, W.V.** (2000) The Adelaide Geosyncline of South Australia and its
814 significance in Neoproterozoic continental reconstruction. *Precambrian Research*,
815 **100**, 21–63.
816
817 **Preiss, W.V., Gostin, V.A., McKirdy, D.M., Ashley, P.M., Williams, G.E. and**
818 **Schmidt, P.W.** (2011) The glacial succession of Sturtian age in South Australia: the
819 Yudnamutana Subgroup. *Geological Society, London, Memoirs*, **36**, 701-712.
820 doi:10.1144/M36.69
821
822 **Prélat, A., Covault, J.A., Hodgson, D.M., Fildani, A. and Flint, S.S.** (2010)
823 Intrinsic controls on the range of volumes, morphologies, and dimensions of
824 submarine lobes. *Sedimentary Geology*, **232**, 66-76.
825 doi:10.1016/j.sedgeo.2010.09.010.
826
827 **Reading, H.G. and Richards, M.** (1994) Turbidite systems in deep-water basin
828 margins classified by grain size and feeder system. *AAPG Bulletin*, **78**, 792-822.
829
830 **Rose, C.V. and Maloof, A.C.** (2010) Testing models for post-glacial ‘cap dolostone’
831 deposition: Nuccaleena Formation, South Australia. *Earth and Planetary Science*
832 *Letters*, **296**, 165–180.
833
834 **Schermerhorn, L. J. G.** (1974) Late Precambrian mixtites: glacial and/or nonglacial.
835 *American Journal of Science*, **274**, 673-824.
836
837 **Schermerhorn, L.J.G. and Stanton, W.I.** (1963) Tilloids in the West Congo Belt.
838 *Quarterly Journal of the Geological Society of London*, **119**, 201-241.
839
840 **Shanmugam, G.** (2002) Ten turbidite myths. *Earth Science Reviews*, **58**, 311-341.
841
842 **Shanmugam, G., Bloch, R.B., Mitchell, S.M., Beamish, G.W.J., Hodgkinson,**
843 **R.J., Damuth, J.E., Staume, T., Syvertsen, S.E. and Shields, K.E.** (1995) Basin-
844 floor fans in the North Sea; sequence stratigraphic models vs. sedimentary facies.
845 *AAPG Bulletin*, **79**, 477-512.
846
847 **Shields, G.A.** (2005) Neoproterozoic cap carbonates: a critical appraisal of existing
848 models and the plumeworld hypothesis. *Terra Nova*, **17**, 299-310.
849
850 **Stokes, C.R. and Clark, C.D.** (2001) Palaeo-ice streams. *Quaternary Science*
851 *Reviews*, **20**, 1437–1457.
852
853 **Taylor, J., Dowdeswell, J.A., Kenyon, N.H. and O’Cofaigh, C.** (2002) Late
854 Quaternary architecture of trough-mouth fans: debris flows and suspended
855 sediments on the Norwegian margin. In: Dowdeswell, J.A., O’Cofaigh, C. (Eds.),
856 Glacier-Influenced Sedimentation on High-Latitude Continental Margins. Special
857 Publication, vol. 203. Geological Society, London, pp. 55–71.

- 858
859 **Thomson, B.P., Coats, R.P., Mirams, R.C., Forbes, B.G., Dalgarno, C.R. and**
860 **Johnson, J.E.** (1964) Precambrian rock groups in the Adelaide Geosyncline: a new
861 subdivision. *Quarterly Geological Notes, Geological Survey of South Australia*, **9**,
862 1-19.
863
864 **Young, G.M. and Gostin, V.A.** (1988) Stratigraphy and Sedimentology of Sturtian
865 glaciogenic deposits in the western part of the North Flinders Basin, South
866 Australia. *Precambrian Research*, **39**, 151–170.
867
868 **Young, G.M. and Gostin, V.A.** (1989) An exceptionally thick upper Proterozoic
869 (Sturtian) glacial succession in the Mount Painter area, South Australia. *Geological*
870 *Society of America Bulletin*, **101** (6), 834–845.
871
872 **Young, G.M. and Gostin, V.A.** (1990) Sturtian glacial deposition in the vicinity of
873 the Yankaninna Anticline, North Flinders Basin, South Australia. *Australian*
874 *Journal of Earth Sciences*, **37**, 447–458.
875
876 **Young, G.M. and Gostin, V.A.** (1991) Late Proterozoic (Sturtian) succession of
877 the North Flinders Basin, South Australia; an example of temperate glaciation in an
878 active rift setting. In: Anderson, J.R., Ashley, G.M. (Eds.), *Glacial Marine*
879 *Sedimentation: Palaeoclimatic Significance. Geological Society of America Special*
880 *Paper*, **261**, 207–222.
881

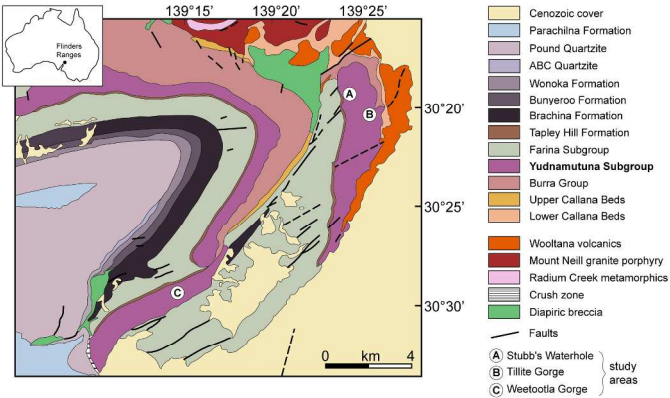


Figure 1: Geological sketch map of the Arkaroola region (modified and simplified after Coats, 1973). Note the location of the Tillite Gorge, Stubb's Waterhole and Weetootla Gorge sections which are shown on figure 4.

210x297mm (300 x 300 DPI)

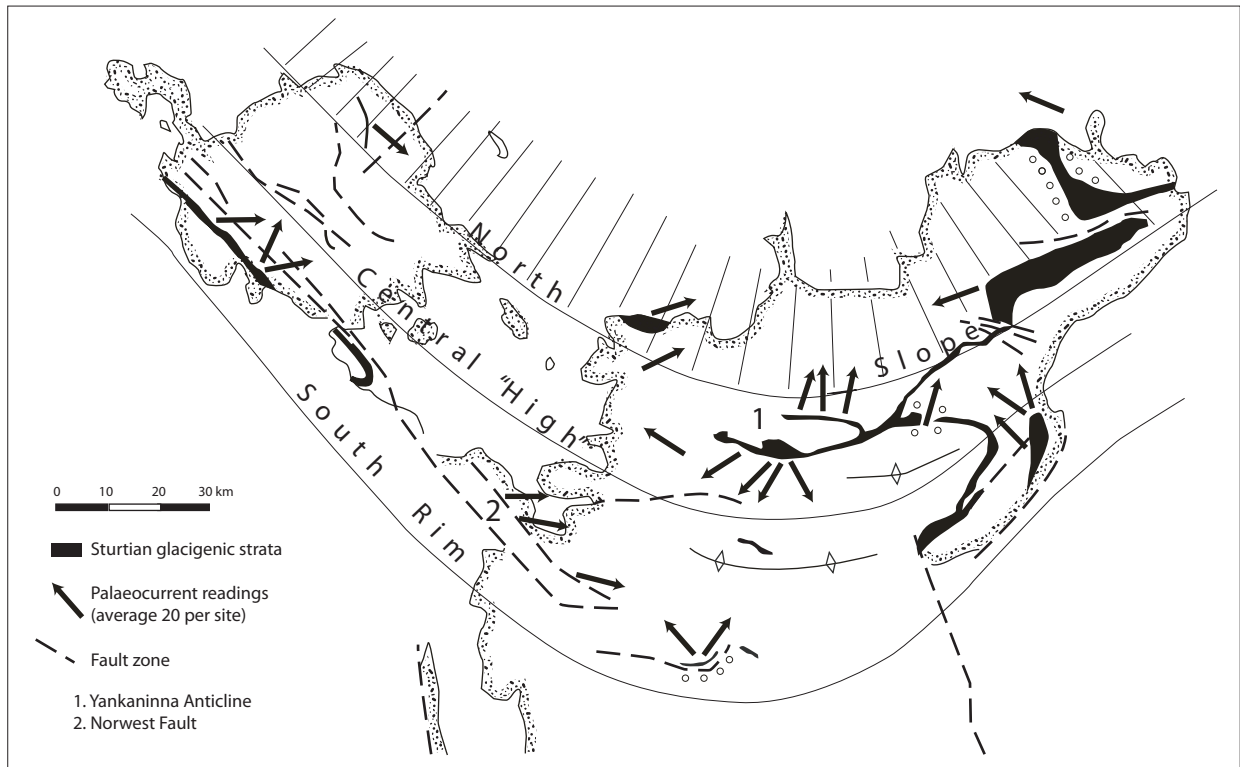


Figure 2

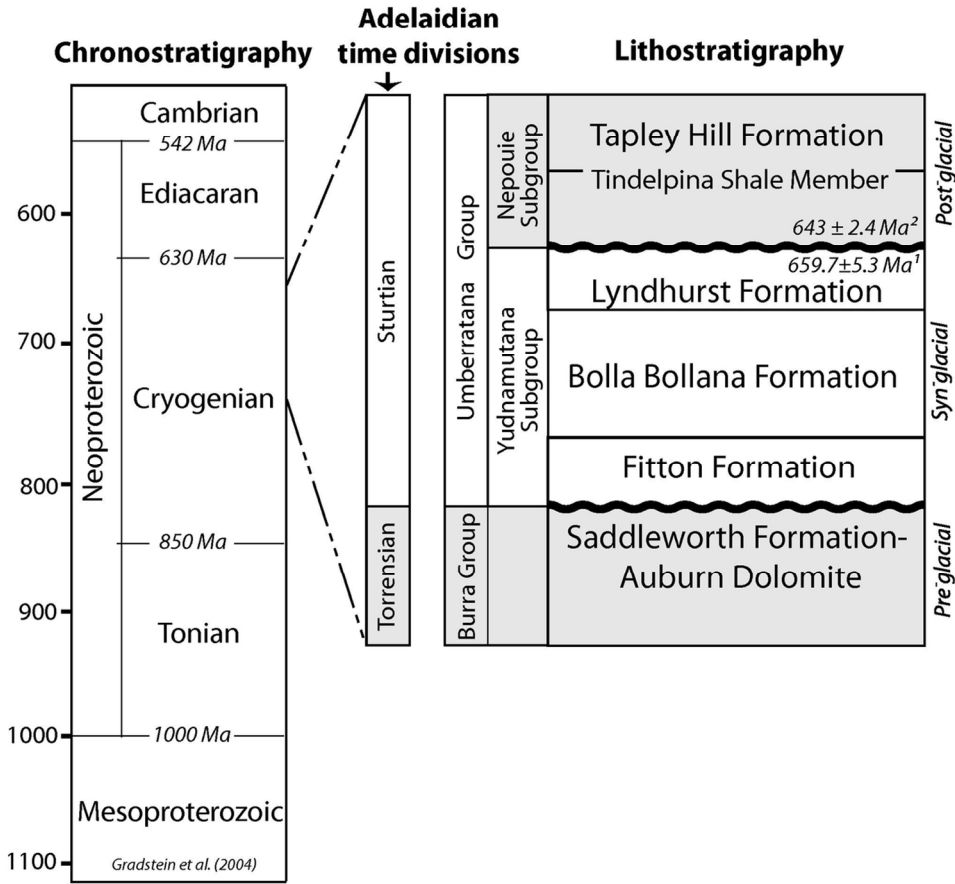


Figure 3: Stratigraphy of the Neoproterozoic of the Arkaroola area, with subdivisions of the Sturt glacial succession based on Young and Gostin (1989). The internal lithostratigraphy of the Sturt glacial succession varies dramatically even over the comparatively small region of the northern Flinders Ranges (c.f. Young and Gostin, 1988, 1989, 1990, 1991). In the Arkaroola district, a threefold division is recognised with the Fitton Formation at the base, the Bolla Bollana Formation in the middle, and the Lyndhurst Formation as the uppermost unit within the Yudnamutana Subgroup. This paper specifically examines the Bolla Bollana Formation.

108x135mm (300 x 300 DPI)

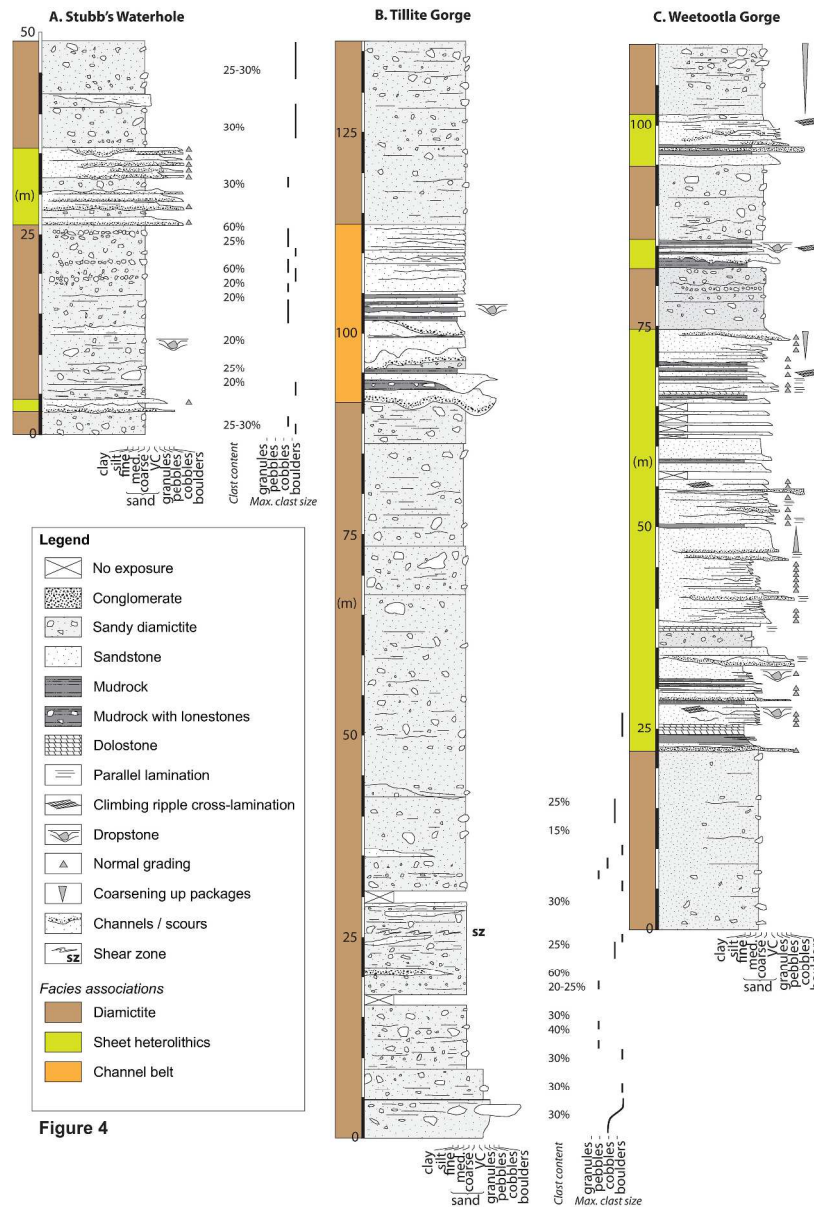


Figure 4

Figure 4: Detailed sedimentary logs through the Bolla Bollana Formation in the Arkaroola district (see Fig. 1 for location of sections). A: Stubb's Waterhole. B: Tillite Gorge. C: Weetootla Gorge. Note that in the case of the diamictites, the grain size in each of the logs refers to grain size of the matrix: maximum clast size, where possible was also measured. These latter data are shown to the right of the logs.

285x422mm (300 x 300 DPI)

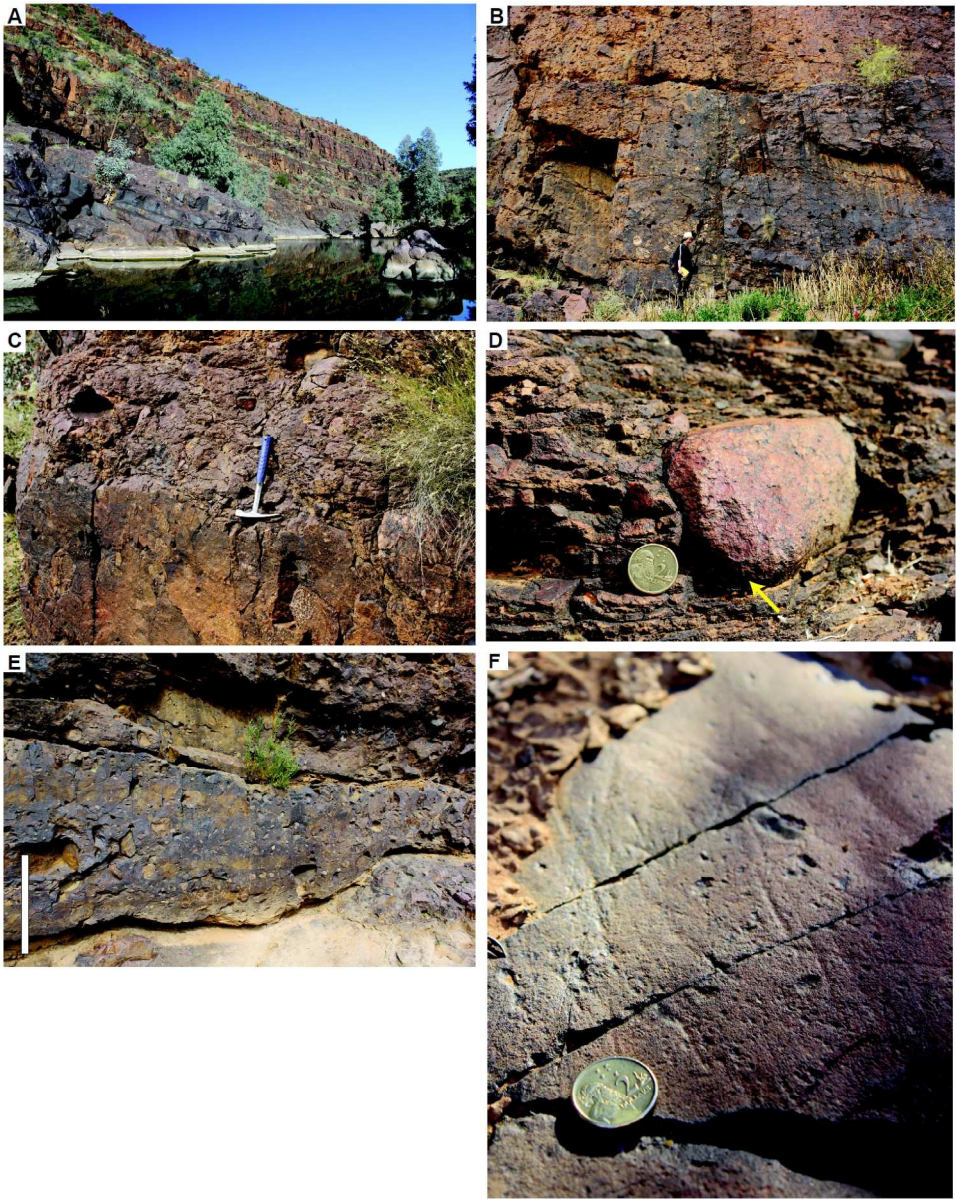


Figure 5: Representative photographs of facies within the diamictite facies association. A: Outcrop perspective of the Tillite Gorge locality, showing thickly bedded diamictites dipping toward the right of the photograph. B: Base of a diamictite megabed (42-67 m, Fig. 4 B) with geologist for scale. C: Clast-poor diamictite overlain by clast-rich diamictite, with geological hammer for scale placed at the boundary. D: Impact structure beneath gneiss pebble in well-stratified diamictite. Rounded clasts are quite typical. E: Undulose contact at the base of a diamictite megabed. Note that this undulose character likely records erosion or differential compaction. Scale bar: 1 m. F: Face of a polished and striated sandstone boulder, showing crosscutting striation orientations.

228x286mm (300 x 300 DPI)

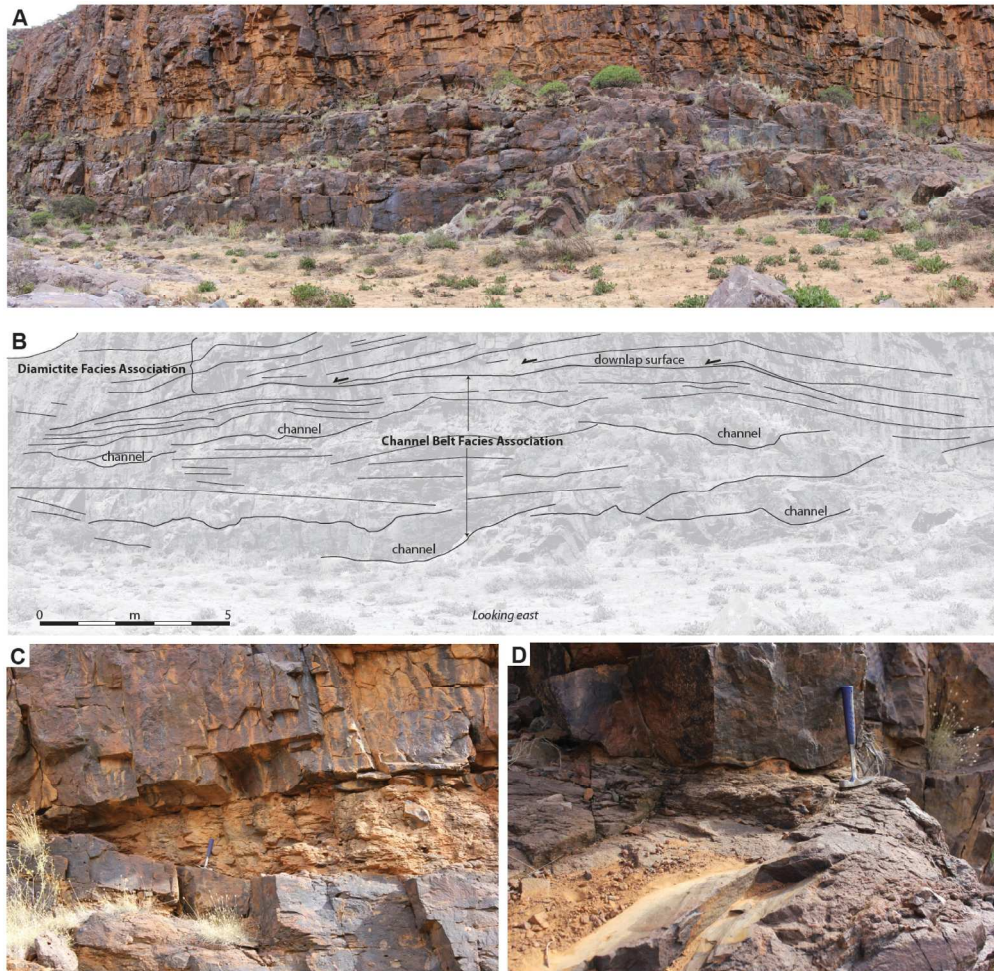


Figure 6: A and B: Panoramic photo and corresponding sketch of stacked channel geometries in the channel belt facies association. Note also the downlapping strata of the diamictite facies association directly above. C: Low angle channel incision cutting down towards the left of the photograph (marked by solid white line), clearly truncating recessive siltstones, themselves infilling a channel scour. D: Low amplitude scour at the base of a sandstone bed: evidence for erosion-based beds even where clear channel geometries are not observed.

187x182mm (300 x 300 DPI)

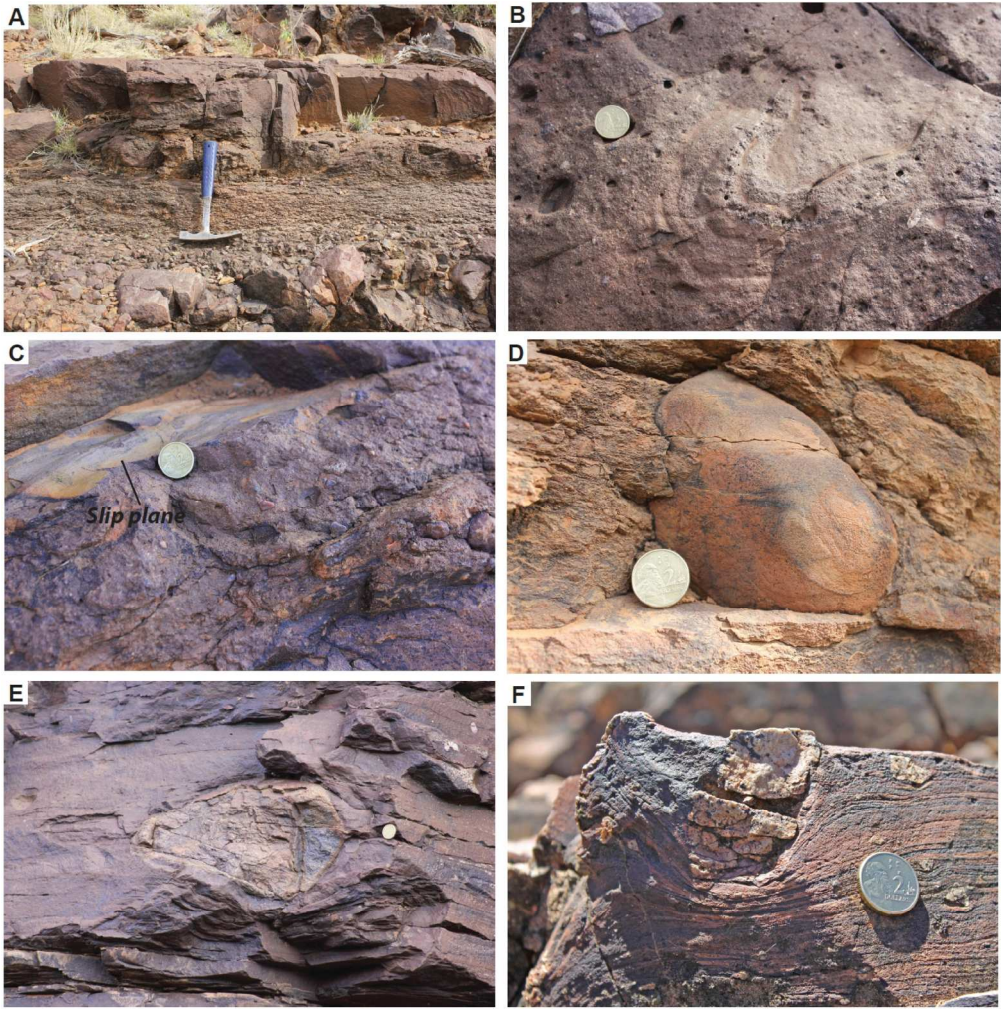


Figure 7: A: Typical fining upward sequence, interpreted as a turbidite bed. In this example, pebble to cobble-grade clasts beneath the hammer pass upward over 10 cm into granular conglomerates, and finally well differentiated, moderately to well-sorted sandstone above the hammer handle. B: Recumbent fold in a turbidite. C: Curvilinear grooves on a sandstone surface, interpreted to record intrastratal shear possibly as a result of compaction, in sandstones. The absence of asperities or quartz/ calcite mineralisation discounts a tectonic origin. D: Striated lonestone within siltstone: a putative dropstone emplaced toward the top of a Bouma sequence. E and F: Two examples of dropstones with clear impact structures in laminated siltstone intervals.

183x185mm (300 x 300 DPI)

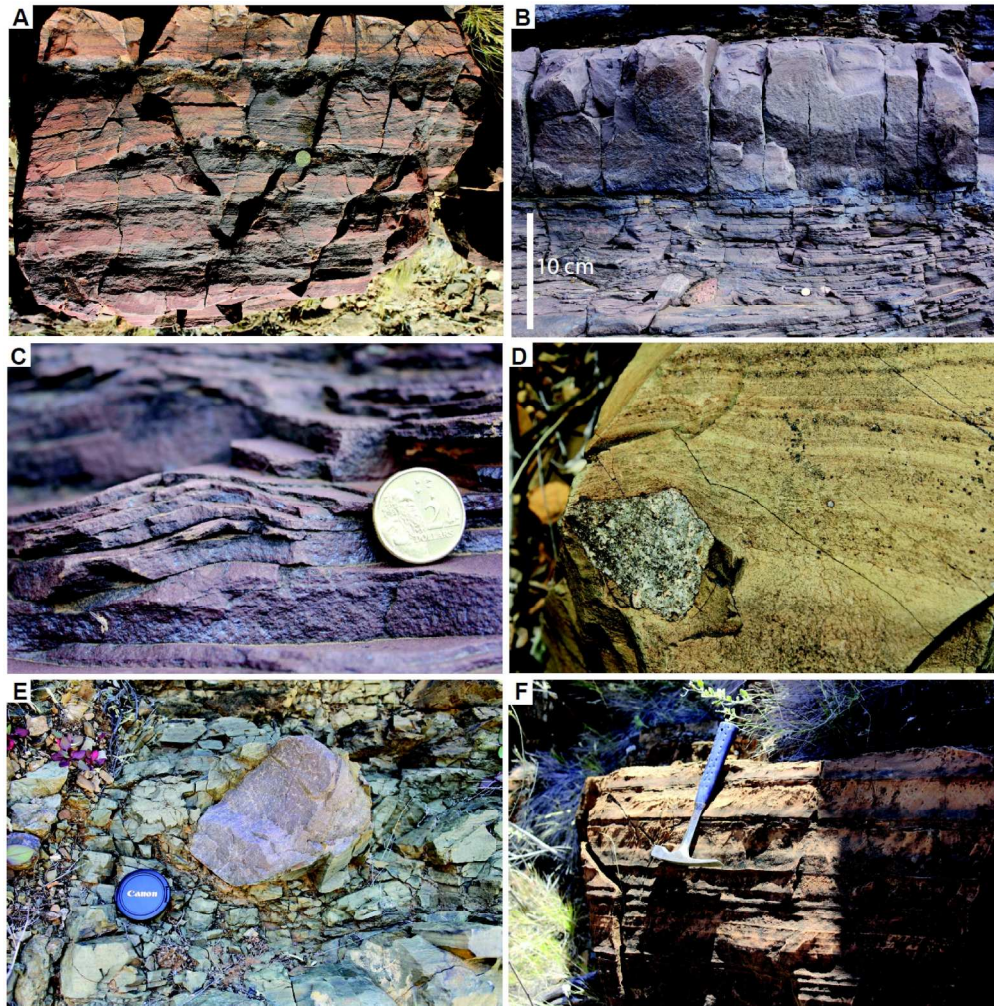


Figure 8: Representative photographs of facies within the sheet heterolithic facies association. A: Repetitively stacked, decimetric Bouma cycles. Note coin for scale. B: Limestones to the left of the coin within fine-grained, climbing ripple cross-laminated sandstone. C: Detail of photo B showing prograding crest (from right to left) of a climbing ripple. Note that tractive velocities predicted within the field of ripple formation (e.g. Bridge and Demicco, 2008) are insufficient to transport pebble-sized clasts. Thus, a dropstone origin is deduced. D: Limestone with deflected laminations above the clast: possibly as a result of compaction. Field of view 7 cm. E: Quartzite dropstone, with impact structure (truncation and piercing of shale laminae) beneath the coin. Laminated dolostone (25 m, Fig. 4 C).

197x198mm (300 x 300 DPI)

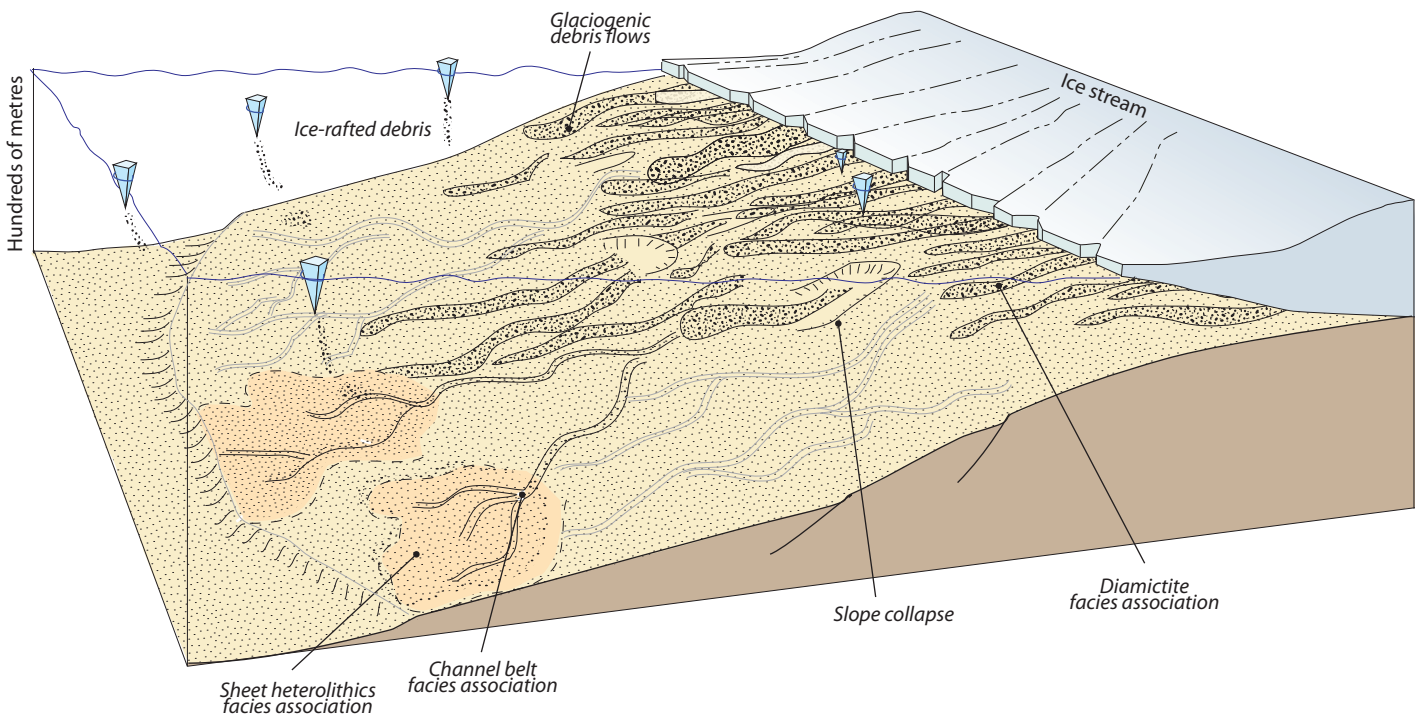


Figure 9